PHYSICAL REVIEW D **94,** 063524 (2016)

Non-Abelian cosmic strings in de Sitter and anti–de Sitter space

Antônio de Pádua Santos[*] and Eugênio R. Bezerra de Mello[†]

Departamento de Física, Universidade Federal da Paraíba, 58.059-970, Caixa Postal 5.008, João Pessoa, Paraíba, Brazil

(Received 21 July 2016; published 20 September 2016)

In this paper we investigate the non-Abelian cosmic string in de Sitter and anti–de Sitter spacetimes. In order to do that we construct the complete set of equations of motion considering the presence of a cosmological constant. By using numerical analysis we provide the behavior of the Higgs and gauge fields and also of the metric tensor for specific values of the physical parameters of the theory. For the de Sitter case, we find the appearance of an horizon. This horizon is consequence of the presence of the cosmological constant, and its position strongly depends on the value of the gravitational coupling. In the anti–de Sitter case, we find that the system does not present horizons. In fact the new feature of this system is related with the behavior of the (00) and (zz) components of the metric tensor. They present a strong increasing behavior for large distance from the string.

DOI: 10.1103/PhysRevD.94.063524

I. INTRODUCTION

Our understanding about the Universe is based upon the standard cosmological model known as the big bang theory. The main feature of the big bang theory is the expansion of the Universe. Under this basis, as the Universe expands it has been cooling. During its cosmological expansion, the Universe underwent a series of phase transitions [1]. These phase transitions are characterized by spontaneously broken gauge symmetries, and they have important roles in the cosmological context [2]. They provide a mechanism for the formation of topological defects that can be described by classical field theories whose configurations of vacuum have elegant and topologically stable solutions with relevant physical implications. Such solutions are specified as the domain wall, monopoles, and cosmic strings, among others [3]. Among them, cosmic strings have been studied most. They can be considered as a candidate to explain the temperature anisotropies of the cosmic microwave background (CMB) [4] and they are associated with the emission of gravitational waves and high-energy cosmic rays [5,6].

Stringlike solutions were obtained by Nielsen and Olesen [7] through a relativistic classical field theory considering a system composed by Abelian and non-Abelain gauge fields coupled with Higgs fields. In the system under consideration, a potential interaction that presents a nontrivial vacuum solution was taken into account. This potential is responsible for the spontaneously breaking of gauge symmetries. The authors were able to find a static, cylindrically symmetric and stable solution from the equations of motion, which corresponds to a magnetic field along the z-direction. This solution was named the "vortex." Unfortunately the complete set of equations associated with this topological object is nonlinear and, in general, there is no closed solution for it. Only asymptotic expressions, for points near or very far from the vortex's core, can be found for the Higgs and gauge fields. A more complex system is formed when one decides to analyze the influence of this linear defect on the geometry of the spacetime. This huge challenge was faced initially by Garfinkle [8] and two years later by Laguna-Castillo and Matzner [9] considering the Abelian version of the Nielsen and Olesen model. The authors have shown that there exists a class of static, cylindrically symmetric solutions of these equations representing a string; moreover, they have showed that these solutions approach asymptotically to a Minkowski spacetime minus a wedge. Linet in [10] analyzed a special kind of Abelian vortex solution that satisfies the Bogomol'nyi-Prasad-Sommerfield (BPS) condition and showed that for the case of an infinite electric charge and Higgs field self-coupling limit, it is possible to obtain exact solutions for the metric tensor, which is determined in terms of the linear energy density of the string.

The analysis of the spacetime geometry in the presence of an infinitely long, straight, static, Abelian cosmic string formed during phase transitions at energy scales larger than the grand-unified-theory scale was developed in [11,12]. For these supermassive configurations, two different types of solutions were found: one [11] in which the components of metric tensor $g_{tt} = g_{zz}$ vanish at finite distance from the axis, and another in which these components remain finite everywhere while $g_{\phi\phi}$ decreases outside the core of the string. Although both types of geometries present different asymptotic behaviors, they are solutions of the same set of differential equations. This apparent contradiction was clarified in the papers [13,14], where the authors pointed out that the coexistence of two different kinds of solutions is a consequence of boundary conditions imposed on the

[*]Present address: Departamento de Física, Universidade Federal Rural de Pernambuco 52.171-900, Recife, Pernambuco, Brazil.
padua.santos@gmail.com
[†]emello@fisica.ufpb.br

metric fields. In fact, the two different kinds of asymptotic behaviors for the metric tensor correspond to the two different branches of cylindrically symmetric vacuum solutions of the Einstein equations [15]. The solution analyzed in [11] corresponds to the so-called Melvin branch, and the case analyzed in [12] corresponds to the so-called string branch. The string branch solutions are those of astrophysical interest, since they describe solutions with a planar angle deficit [16]; moreover, the Melvin branch has no flat spacetime counterpart. In [17] it was discussed how the presence of multiple supermassive cosmic strings in the Abelian model can induce the spontaneous compactification of the transverse space to a cosmic string and to construct solutions where the gravitational background becomes regular everywhere.

In general relativity, de Sitter (dS) and anti–de Sitter (AdS) spacetimes are maximally symmetric solutions of Einstein's field equations in the presence of a positive and negative cosmological constant, Λ, respectively. Due to the symmetry of de Sitter and anti–de Sitter spacetimes, numerous physical problems have been exactly solved. In particular, astronomical observations of high redshift supernovae, galaxy clusters, and the cosmic microwave background [18,19] indicate that during the present epoch in which we live, the Universe may be described by de Sitter spacetime. On the other hand, anti–de Sitter spacetime plays an important role in theoretical physics such as the realization of the holographic principle known as AdS/CFT correspondence [20]. So, in the context of a gravitating local cosmic string, a natural question takes place: how does the presence of the cosmological constant, positive or negative, modify the geometry of the spacetime produced by an Abelian or non-Abelian cosmic string? The answer to this question is the main objective of the present analysis.

In fact, the numerical analysis of the Abelian Nielsen and Olesen string minimally coupled to gravity including a positive cosmological constant has been studied in [21]. Moreover, the analysis of Abelian strings in a fixed background spacetime with positive cosmological constant has been investigated in [22,23]. In addition, the spherically symmetric topological defect named the global monopole [24] was investigated in dS and AdS spacetimes by Li and Hao in [25] and by Bertrand *et al.* in [26].

In the paper by Nielsen and Olesen, the non-Abelian string system was described by an $SU(2)$ gauge invariant Lagrangian density composed of gauge fields and two Higgs sectors. A potential responsible for the spontaneously broken gauge symmetry was present. The analysis of the non-Abelian Nielsen and Olesen string and its influence on the geometry of the spacetime was only recently considered in [27]. In this analysis, the presence of a cosmological constant was not taken into account. All the modifications in the Minkowski spacetime were caused by the defect. So, as an additional motivation to develop this work, we would like to complete this analysis considering now that the non-Abelian string, and also the Abelian one, is in dS and AdS spacetimes.

This paper is organized as follows: In Sec. II we present the non-Abelian Higgs model in de Sitter and anti–de Sitter spaces and analyze the conditions that the physical parameters contained in the potential should satisfy so that the system presents stable topological solutions. Also we present the ansatz for the Higgs and gauge fields and for the metric tensor. The equations of motion and boundary conditions are presented in Sec. III. In Sec. IV we provide our numerical results, exhibiting the behaviors of the Higgs, gauge, and metric fields as functions of the distance to the core of the string. Moreover, we present a comparison of the non-Abelian system in Minkowski, de Sitter, and anti–de Sitter spaces, and point out the most relevant aspects that distinguish the behaviors of those fields in the presence/absence of a cosmological constant. Finally in Sec. V we give our conclusions.

II. THE MODEL

In a previous work [27], we studied the behavior of gravitating non-Abelian strings in the absence of a cosmological constant. We mainly considered the planar angle deficit in the spacetime caused by the string and the energy density by unit length associated with this system, and we compared both quantities, separately, with the corresponding ones for the Abelian string. The aim of this paper is to examine the influence of the cosmological constant in the non-Abelian and Abelian cosmic string spacetimes. For the present purposes, we introduce the cosmological constant in the model described by the following action, S:

$$S=\int d^4x\sqrt{-g}\left(\frac{1}{16\pi G}(R-2\Lambda)+\mathcal{L}_m\right), \tag{2.1}$$

where R is the Ricci scalar, G denotes the Newton's constant, and Λ is the cosmological constant.[1] The matter Lagrangian density of the non-Abelian Higgs model is given by

$$\mathcal{L}_m=-\frac{1}{4}F^a_{\mu\nu}F^{\mu\nu a}+\frac{1}{2}(D_\mu\varphi^a)^2+\frac{1}{2}(D_\mu\chi^a)^2 - V(\varphi^a,\chi^a), a=1,2,3, \tag{2.2}$$

where $F^a_{\mu\nu}$ denotes the field strength tensor,

$$F^a_{\mu\nu}=\partial_\mu A^a_\nu-\partial_\nu A^a_\mu+e\epsilon^{abc}A^b_\mu A^c_\nu. \tag{2.3}$$

The covariant derivative is given by $D_\mu\varphi^a=\partial_\mu\varphi^a+e\epsilon^{abc}A^b_\mu\varphi^c$, where the latin indices denote the internal gauge groups. A^b_μ is the $SU(2)$ gauge potential and e the

[1]For de Sitter space $\Lambda>0$ and for anti–de Sitter space $\Lambda<0$.

gauge coupling constant. The interaction potential, $V(\varphi^a,\chi^a)$, is defined by the expression

$$V(\varphi^a,\chi^a)=\frac{\lambda_1}{4}[(\varphi^a)^2-\eta_1^2]^2+\frac{\lambda_2}{4}[(\chi^a)^2-\eta_2^2]^2+\frac{\lambda_3}{2}[(\varphi^a)^2-\eta_1^2][(\chi^a)^2-\eta_2^2], \tag{2.4}$$

where the λ_1 and λ_2 are the Higgs fields self-coupling positive constants and λ_3 is the coupling constant between both bosonic sectors. η_1 and η_2 are parameters corresponding to the energy scales where the gauge symmetry is broken. The potential above has different properties according to the sign of $\Delta\equiv\lambda_1\lambda_2-\lambda_3^2$ [27]:

(i) For $\Delta>0$, the potential has positive value and its minimum is attained for $(\varphi^a)^2=\eta_1^2$ and $(\chi^a)^2=\eta_2^2$.

(ii) For $\Delta<0$, these configurations lead to saddle points and two minima occur for

$$(\varphi^a)^2=0,\qquad (\chi^a)^2=\eta_2^2+\frac{\lambda_3}{\lambda_2}\eta_1^2 \tag{2.5}$$

and

$$(\chi^a)^2=0,\qquad (\varphi^a)^2=\eta_1^2+\frac{\lambda_3}{\lambda_1}\eta_2^2. \tag{2.6}$$

The values of the potential for these cases are, respectively,

$$V_{\min}=\frac{\eta_1^4}{4\lambda_2}\Delta\quad\text{and}\quad V_{\min}=\frac{\eta_2^4}{4\lambda_1}\Delta. \tag{2.7}$$

Both values for $V_{\min}$ are negatives, since $\Delta<0$.

A. The ansatz

First let us consider the most general, cylindrically symmetric line element invariant under boosts along the z-direction. By using cylindrical coordinates, this line element is given by

$$ds^2=N^2(\rho)dt^2-d\rho^2-L^2(\rho)d\phi^2-N^2(\rho)dz^2. \tag{2.8}$$

For this metric, the nonvanishing components of the Ricci tensor, $R_{\mu\nu}$, are

$$R_{tt}=-R_{zz}=\frac{NLN''+NN'L'+L(N')^2}{L}, \tag{2.9}$$

$$R_{\rho\rho}=\frac{2LN''+NL''}{NL}, \tag{2.10}$$

$$R_{\phi\phi}=\frac{L(2N'L'+NL'')}{N}, \tag{2.11}$$

where the primes denotes derivative with respect to ρ.

For the Higgs and gauge fields we have the following expressions [28]:

$$\varphi^a(\rho)=f(\rho)\begin{pmatrix}\cos(\phi)\\ \sin(\phi)\\ 0\end{pmatrix}, \tag{2.12}$$

$$\chi^a(\rho)=g(\rho)\begin{pmatrix}-\sin(\phi)\\ \cos(\phi)\\ 0\end{pmatrix}, \tag{2.13}$$

$$\vec{A}^a(\rho)=\hat{\phi}\left(\frac{1-H(\rho)}{e\rho}\right)\delta_{a,3} \tag{2.14}$$

and

$$A_t^a(\rho)=0,\qquad a=1,2,3. \tag{2.15}$$

From the above expressions, we can see that both isovector bosonic fields satisfy the orthogonality condition, $\varphi^a\chi^a=0$.

III. EQUATION OF MOTION

In this paper we shall use the same notation as in [27] for the dimensionless variables and functions, as shown below:

$$x=\sqrt{\lambda_1}\eta_1\rho,\qquad f(\rho)=\eta_1 X(x),\qquad g(\rho)=\eta_1 Y(x),\qquad L(x)=\sqrt{\lambda_1}\eta_1 L(\rho). \tag{3.1}$$

Adopting these notations, the Lagrangian density will depend only on dimensionless variables and parameters:

$$\alpha=\frac{e^2}{\lambda_1},\qquad q=\frac{\eta_1}{\eta_2},\qquad \beta_i^2=\frac{\lambda_i}{\lambda_1},\quad i=1,2,3,\qquad \gamma=\kappa\eta_1^2,\qquad \bar{\Lambda}=\frac{\Lambda}{\eta_1^2\lambda_1}\quad\text{and}\quad \kappa=8\pi G. \tag{3.2}$$

For the de Sitter or anti–de Sitter spacetime, it is convenient to use the Einstein field equations in the form

$$R_{\mu\nu}=-\kappa\left(T_{\mu\nu}-\frac{1}{2}g_{\mu\nu}T\right)+\Lambda g_{\mu\nu},\quad\text{with}\quad T=g^{\mu\nu}T_{\mu\nu}\quad\text{and}\quad \mu,\nu=t,x,\phi,z. \tag{3.3}$$

For the energy-momentum tensor associated with the matter field we use the usual definition given below,

$$T_{\mu\nu} = \frac{2}{\sqrt{-g}}\frac{\delta S}{\delta g^{\mu\nu}}, \qquad g = \det(g_{\mu\nu}). \tag{3.4}$$

Varying the action (2.1) with respect to matter fields, we obtain the Euler-Lagrange equations below:

$$\frac{(N^2LX')'}{N^2L} = X\left[X^2 - 1 + \beta_3^2(Y^2 - q^2) + \frac{H^2}{L^2}\right], \tag{3.5}$$

$$\frac{(N^2LY')'}{N^2L} = Y\left[\beta_3^2(X^2 - 1) + \beta_2^2(Y^2 - q^2) + \frac{H^2}{L^2}\right], \tag{3.6}$$

$$\frac{L}{N^2}\left(\frac{N^2H'}{L}\right)' = \alpha(X^2 + Y^2)H. \tag{3.7}$$

As for the Einstein equations (3.3), we obtain

$$\frac{(LNN')'}{N^2L} = -\bar{\Lambda} + \gamma\left[\frac{H'^2}{2\alpha L^2} - \frac{1}{4}(X^2-1)^2 - \frac{\beta_2^2}{4}(Y^2-q^2)^2 - \frac{\beta_3^2}{2}(X^2-1)(Y^2-q^2)\right] \tag{3.8}$$

and

$$\frac{(N^2L')'}{N^2L} = -\bar{\Lambda} - \gamma\left[\frac{H'^2}{2\alpha L^2} + (X^2+Y^2)\frac{H^2}{L^2} + \frac{1}{4}(X^2-1)^2 + \frac{\beta_2^2}{4}(Y^2-q^2)^2 + \frac{\beta_3^2}{2}(X^2-1)(Y^2-q^2)\right]. \tag{3.9}$$

The primes in Eqs. (3.5)–(3.9) stand for derivatives with respect to x. As we can see, this set of nonlinear coupled differential equations is a difficult system to analyze. We shall leave this task for the next section. Defining $u = \sqrt{-g} = N^2L$, we obtain the following equation:

$$\frac{u''(x)}{u(x)} = -3\bar{\Lambda} - \gamma\left[-\frac{H'^2}{2\alpha L^2} + (X^2+Y^2)\frac{H^2}{L^2} + \frac{3}{4}(X^2-1)^2 + \frac{3\beta_2^2}{4}(Y^2-q^2)^2 + \frac{3\beta_3^2}{2}(X^2-1)(Y^2-q^2)\right]. \tag{3.10}$$

Before finishing this subsection, we would like to point out that the set of differential equations above reduces itself to the corresponding one for the Abelian Higgs model by taking $\beta_2 = \beta_3 = 0$ and setting one of the Higgs fields equal to zero. Because one of our objectives is to compare the non-Abelian results with the corresponding one for the Abelian case, we shall take, when necessary, the bosonic field $\chi = 0$, which, in terms of dimensionless functions, corresponds to taking $Y = 0$.

A. Boundary conditions

The boundary conditions imposed on the fields at the origin are determined by the requirements of regularity at this point. However, the sign of the cosmological constant, $\bar{\Lambda}$, will establish different kinds of boundary conditions for the matter and gauge fields at large distances.

(i) For de Sitter space ($\bar{\Lambda} > 0$), the boundary conditions for the matter and gauge fields are

$$H(0) = 1, \qquad X(0) = 0, \qquad Y(0) = 0. \tag{3.11}$$

As we shall see, the cosmological constant will provide a cosmological horizon for the metric tensor. Then we must integrate the equations until we obtain this value of the coordinate, $x = x_0$, in order to have the core of the cosmic string located inside the horizon. So, we require

$$X(x = x_0) = 1, \qquad Y(x = x_0) = \frac{\eta_2}{\eta_1} = q, \qquad H(x = x_0) = 0. \tag{3.12}$$

(ii) For anti–de Sitter space ($\bar{\Lambda} < 0$), the cosmological horizon does not appear. Therefore the boundary conditions for the matter and gauge fields are

$$H(0) = 1; \qquad H(\infty) = 0, \tag{3.13}$$

$$X(0) = 0, \qquad X(\infty) = 1, \qquad Y(0) = 0, \qquad Y(\infty) = \frac{\eta_2}{\eta_1} = q. \tag{3.14}$$

The boundary conditions for the metric fields are

$$N(0) = 1, \qquad N'(0) = 0, \qquad L(0) = 0, \qquad L'(0) = 1 \tag{3.15}$$

in both spaces.

B. Vacuum solution

The vacuum solution of our system is attained by setting $X(x) = 1$, $Y(x) = q$, and $H(x) = 0$ in Eq. (3.10). So, we have

(i) For de Sitter spacetime ($\bar{\Lambda} > 0$), we get

$$N^2(x)L(x) = A_1\sin(\sqrt{3\bar{\Lambda}}x) + B_1\cos(\sqrt{3\bar{\Lambda}}x). \tag{3.16}$$

Using the boundary condition Eq. (3.15), we find the following solution:

$$N^2(x)L(x) = \frac{1}{\sqrt{3\bar{\Lambda}}}\sin(\sqrt{3\bar{\Lambda}}x). \tag{3.17}$$

Following the method suggested by Linet [29], we find the solutions

$$N(x) = \cos^{2/3}\left(\sqrt{3\bar{\Lambda}}\frac{x}{2}\right) \tag{3.18}$$

and

$$L(x) = \frac{2^{2/3}}{\sqrt{3\bar{\Lambda}}}\left[\sin(\sqrt{3\bar{\Lambda}}x)\right]^{1/3}\left[\tan\left(\sqrt{3\bar{\Lambda}}\frac{x}{2}\right)\right]^{2/3}. \tag{3.19}$$

(ii) For anti–de Sitter spacetime ($\bar{\Lambda} < 0$), we get

$$N^2(x)L(x) = A_2\exp(\sqrt{3|\bar{\Lambda}|}x) + B_2\exp(-\sqrt{3|\bar{\Lambda}|}x). \tag{3.20}$$

Using the boundary condition Eq. (3.15), we find the following solution:

$$N^2(x)L(x) = \frac{1}{\sqrt{3|\bar{\Lambda}|}}\sinh(\sqrt{3|\bar{\Lambda}|}x). \tag{3.21}$$

By means of [29], we find the solutions

$$N(x) = \cosh^{2/3}\left(\sqrt{3|\bar{\Lambda}|}\frac{x}{2}\right) \tag{3.22}$$

and

$$L(x) = \frac{2^{2/3}}{\sqrt{3|\bar{\Lambda}|}}\left[\sinh(\sqrt{3|\bar{\Lambda}|}x)\right]^{1/3} \times\left[\tanh\left(\sqrt{3|\bar{\Lambda}|}\frac{x}{2}\right)\right]^{2/3}. \tag{3.23}$$

Here we would like to point out that naturally a cosmological horizon takes place in de Sitter spacetime. In the vacuum conditions, the cosmological horizon appears at the first zero of $N(x)$. This occurs at $x_0^v = \frac{\pi}{\sqrt{3\bar{\Lambda}}}$. At the same position, $L(x \to x_0^v) \to \infty$. We also want to mention that the singular behavior of the functions $N(x)$ and $L(x)$ near x_0^v is similar to the singular behavior of the corresponding components of the metric tensor associated with the supermassive configuration analyzed in [11]. Near their corresponding singular point, these functions behave as

$$N(x) \approx (x_{\text{sing}} - x)^{2/3} \quad \text{and} \quad L(x) \approx (x_{\text{sing}} - x)^{-1/3}. \tag{3.24}$$

However we would like to emphasize that the physical reasons for both singular behaviors are different. The source of the singular behavior found in [11] is a supermassive configuration of matter fields. Here is the presence of a positive cosmological constant. As for the anti–de Sitter spacetime, there is no cosmological horizon.

Although the above analysis present important information about the behaviors of the metric fields N and L, we expect that the nontrivial structures of the Higgs and gauge fields produce relevant modifications on these behaviors.[2] We leave this analysis for the next section.

IV. NUMERICAL SOLUTIONS

In this section we shall analyze numerically our system. To do that we integrate numerically Eqs. (3.5)–(3.9) with the appropriated boundary conditions specified in (3.11)–(3.15), corresponding to the dS and AdS cases, by using the ordinary differential equation (ODE) solver COLSYS [30]. Relative errors of the functions are typically of the order of 10^{-8} to 10^{-10} (and sometimes even better).

Our objective is to analyze the behavior of the solutions of the non-Abelian cosmic string in de Sitter and anti–de Sitter spacetime. In order to do this, we construct solutions by specifying the set of physical parameters of the system for positive (de Sitter spacetime) and negative (anti–de Sitter spacetime) values of the cosmological constant, $\bar{\Lambda}$. Moreover, we are also interested in comparing these behaviors with the corresponding one for the Abelian gravitating strings, observing, separately, the influence of each system on the geometry of the spacetime.

A. de Sitter spacetime

In the first moment, we shall analyze the behaviors of Higgs, gauge, and metric fields for the non-Abelian cosmic strings in de Sitter spacetime. Our results for the non-Abelian case are shown in Fig. 1. In the left plot we present the Higgs fields, X and Y, and gauge field, H, as functions of x. In the right plot we present the behavior of the metric functions, N and L. In both plots we set the parameters as $\alpha = 0.8$, $\gamma = 0.61$, $\bar{\Lambda} = 0.0075$, $\beta_2 = 2.0$, $\beta_3 = 1.0$, and $q = 1.0$.

In Fig. 2 we present the behavior of the Higgs and gauge fields, and the metric functions for the Abelian case in de Sitter spacetime. In the left plot, we exhibit the Higgs and gauge fields, X and H, respectively, as functions of the dimensionless variable x. In the right plot we present the metric functions, N and L, as functions of x. For both plots we consider the parameters $\alpha = 0.8$, $\gamma = 0.61$, and $\bar{\Lambda} = 0.0075$.

By comparing Fig. 1(b) with Fig. 2(b), it can be seen that both systems present cosmological horizons, x_0. Moreover, the corresponding values for the horizons for the

[2]Specifically in the Minkowski spacetime, it is well known that the Abelian and also non-Abelian strings produce significant modifications in the geometry when compared with vacuum. The most relevant one is associated with the decreasing slope of L causing a planar angle deficit.

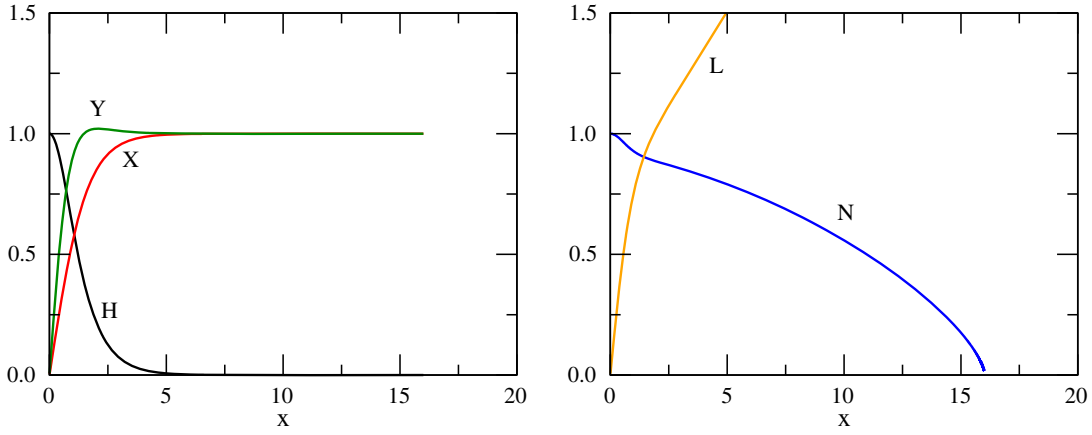

FIG. 1. Non-Abelian string. Left: Behavior for the Higgs and gauge fields as functions of x. Right: Behavior of the metric functions as functions of x. In both plots we consider the parameters $\alpha = 0.8$, $\gamma = 0.61$, $\bar{\Lambda} = 0.0075$, $\beta_2 = 2.0$, $\beta_3 = 1.0$, and $q = 1.0$.

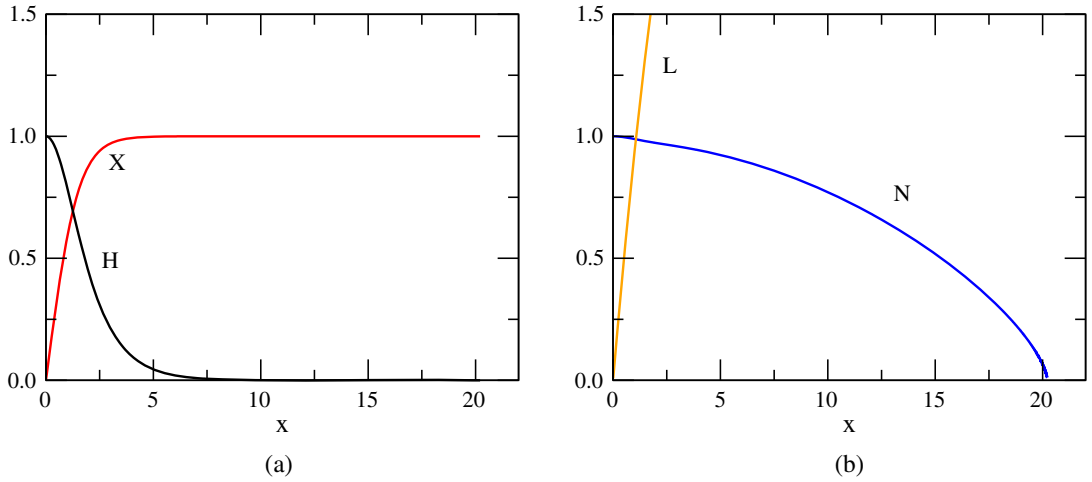

FIG. 2. Abelian string. Left: Behavior for the Higgs and gauge fields as functions of x. Right: Behavior of the metric functions as functions of x. In both plots we consider the parameters $\alpha = 0.8$, $\gamma = 0.61$, $\bar{\Lambda} = 0.0075$.

non-Abelian system are smaller than the Abelian one. Another point that can be mentioned is that, for values of the parameters that we have chosen, the matter fields and gauge fields reach their asymptotic values in the region inside the horizons.

In the vacuum solution we have found that the cosmological horizon is reached for $x_0^v = \frac{\pi}{\sqrt{3\bar{\Lambda}}}$, which for the value of the cosmological constant adopted in the plots, provides $x_0^v \approx 20.94395$. More realistic values for the cosmological horizons were obtained in both plots, considering the nontrivial behaviors of the fields. Motivated by this fact, now we want to investigate how the cosmological horizon depends on the gravitational coupling, γ, and also on the cosmological constant itself, $\bar{\Lambda}$.

First we consider the dependence of x_0 with γ. In order to make this analysis we fixed $\alpha, \beta_2, \beta_3, \bar{\Lambda}$, and q. The value of the cosmological horizon is obtained when the metric function $N(x = x_0)$ is zero. Our numerical results for $\alpha = 0.8, \beta_2 = 2.0, \beta_3 = 1.0, \bar{\Lambda} = 0.0075$, and $q = 1.0$ are presented in Fig. 3(a). Note that the cosmological horizon decreases as the value of γ increases.

As for the influence of $\bar{\Lambda}$ on the cosmological horizon, we adopted a similar procedure to the case above. Nevertheless we fixed α, γ, β_2, β_3, and q, and we determined the value of x at which $N(x)$ vanishes. Our results are presented in Fig. 3(b). We clearly note that the value of the cosmological constant decreases as the value of $\bar{\Lambda}$ increases. Also in this plot, we provide the behaviour for the cosmological horizon in the vacuum case.

B. Anti–de Sitter spacetime

Here, we are interested to analyze the influence of a negative cosmological constant on the behavior of the non-Abelian and Abelian cosmic string systems.

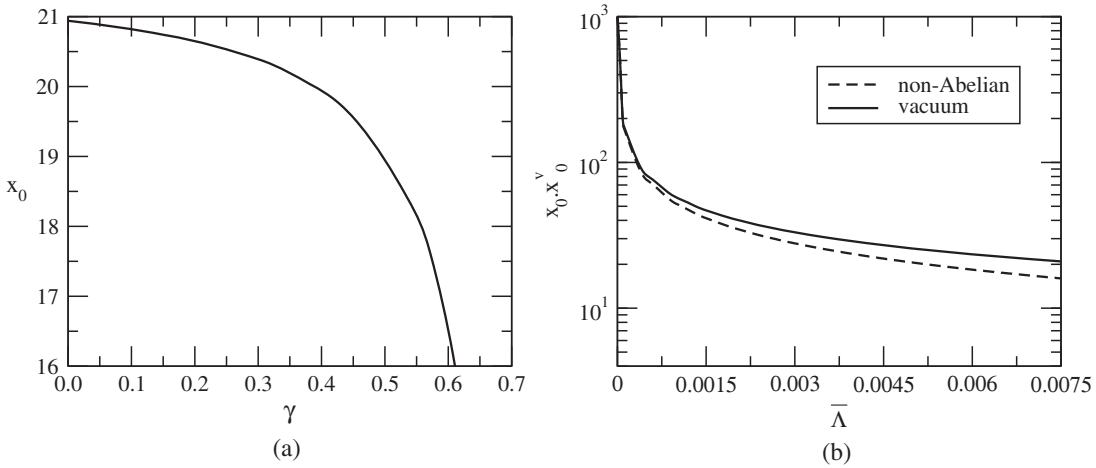

FIG. 3. (a) The behavior of the cosmological horizon, x_0, as a function of γ considering the parameters $\alpha = 0.8, \beta_2 = 2.0, \beta_3 = 1.0, \bar{\Lambda} = 0.0075, q = 1.0$. (b) The dashed line represents the behavior of the cosmological horizon, x_0, as a function of $\bar{\Lambda}$ for the non-Abelian string case, considering $\alpha = 0.8, \gamma = 0.61, \beta_2 = 2.0, \beta_3 = 1.0, q = 1.0$. The solid line corresponds to the trivial behavior of the cosmological horizon, x_o^v, in the vacuum case.

In Fig. 4(a) we present the behavior of the Higgs fields, X and Y, and gauge field, H, for the non-Abelian case as functions of the dimensionless variable x, considering specific values attributed to the set of parameters. In Fig. 4(b) we plot the behavior of the corresponding metric functions, N and L, as functions of x. In both plots we considered the parameters $\alpha = 0.8, \gamma = 0.6, \beta_2 = 2.0, \beta_3 = 1.0, \bar{\Lambda} = -0.03$, and $q = 1.0$.

In Fig. 5(a) we present the behavior of the Higgs field, X, and gauge field, H, in the Abelian case for specific values attributed to the set of appropriated parameters. In Fig. 5(b) we plot the metric functions, N and L. In both plots we consider the parameters for the Abelian case as $\alpha = 0.8$, $\gamma = 0.6$, and $\bar{\Lambda} = -0.03$. For both systems we can see that the function N presents a strong increment for large value of x.

Finally we present in Fig. 6 the behavior of the metric fields for two different values of the cosmological constant, $\bar{\Lambda} = -0.010$ and $\bar{\Lambda} = -0.007$, in the non-Abelain case with parameters $\alpha = 0.8, \gamma = 0.6, \beta_2 = 2.0, \beta_3 = 1.0$, and $q = 1.0$. We notice that the metric field N increases with the cosmological constant.

C. Comparative analysis

In this section we would like to present plots comparing the behaviors of the metric fields, $L(x)$ and $N(x)$, as functions of x for different background spacetimes: (a) the non-Abelian cosmic sting in Minkowski (M) and in de Sitter (dS) spacetimes, and (b) the non-Abelian cosmic string in Minkowski (M) and anti–de Sitter (AdS) spacetimes. In addition we have included the behaviors of these metric functions in the vacuum (vac) for dS and AdS

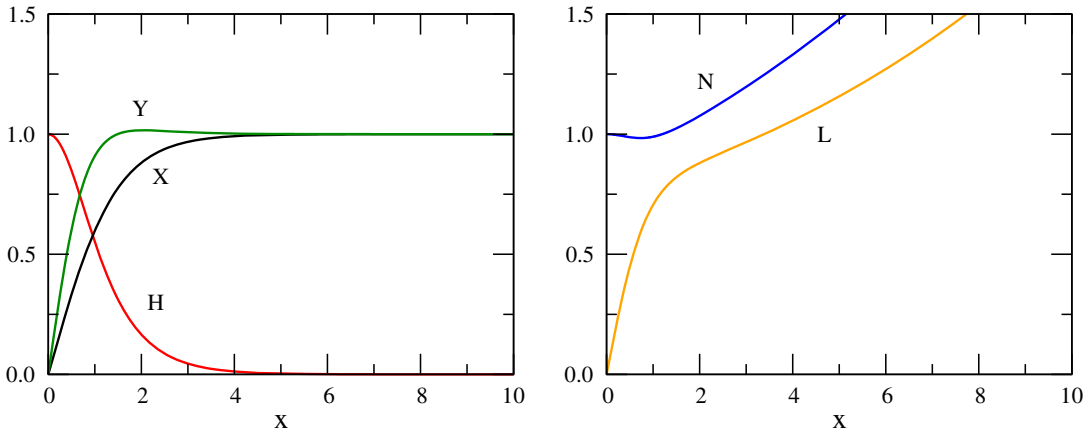

FIG. 4. Non-Abelian string. Left: Behavior of the Higgs and gauge fields in anti–de Sitter space. Right: Metric functions. In both plots we have considered $\alpha = 0.8, \gamma = 0.6, \beta_2 = 2.0, \beta_3 = 1.0, \bar{\Lambda} = -0.03$, and $q = 1.0$.

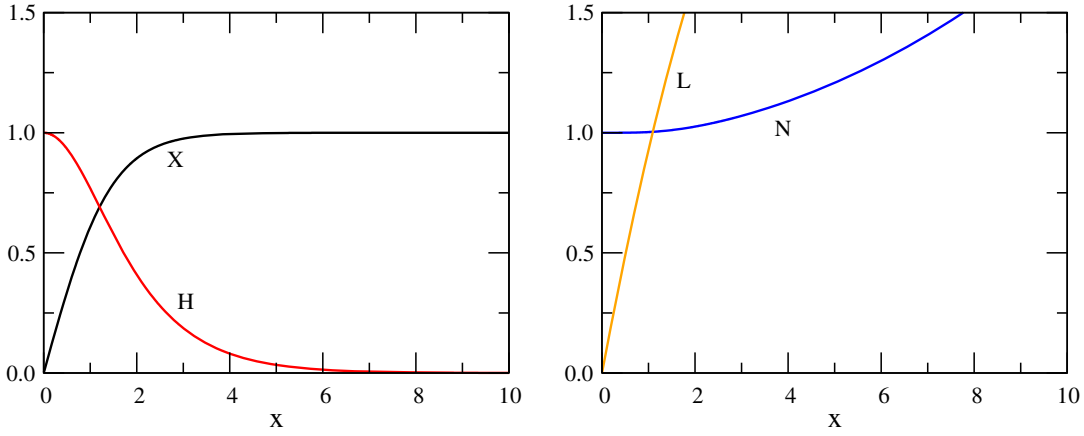

FIG. 5. Abelian string. Left: Behavior of the Higgs and gauge fields in anti–de Sitter space as functions of x. Right: Behavior of the metric fields in anti–de Sitter space considering $\alpha = 0.8, \gamma = 0.6, \bar{\Lambda} = -0.03$.

spacetimes, given by Eqs. (3.18), (3.19), (3.22), and (3.23). In the plots we label these curves with the subscripts M, dS, AdS, and vac, according to the space background considered. In this way we intend to point out the most relevant aspects that distinguish the behaviors of those functions. In our analysis presented in Fig. 7, we adopted the following values for the parameters: $\gamma = 0.6, \alpha = 0.8, \beta_2 = 2.0$, $\beta_3 = 1.0$, and $q = 1.0$. For dS space we take $\bar{\Lambda} = 0.0075$ and for AdS we take $\bar{\Lambda} = -0.03$. The behaviors of the Higgs and gauge fields are almost insensitive to the presence of a cosmological constant; for this reason we decided not to include them in the plots.

In Fig. 7(a) we present the behaviors of L and N as functions of x considering the non-Abelian cosmic string in Minkowski and de Sitter spacetimes. Also we present their behaviors in vacuum de Sitter space, named vacuum solutions. We can see that the main difference is in the behaviors of the component N. In Minkowski space, this component tends to be a constant value below unity while in dS space it goes to zero. In addition, comparing N in dS with N in the vacuum, we can see that the cosmological horizon for the first case is smaller than that for the second one. A less evident difference is in the behavior of L. Comparing the plot of this component in the vacuum, L_{vac}, in the non-Abelian string in dS, L_{dS}, and non-Abelian string in Minkowski, L_M, spacetimes, respectively, we can notice a progressive bending. Specifically there is a small deviation between L_{dS} and L_M. Another point that deserves to be mentioned is the decreasing slope of L when one compares L_{vac} with L_{dS}. The slope of the latter is smaller for any given point. This resembles the decreasing in the slope of L_M when compared with the one in the vacuum in Minkowski spacetime. In fact, by comparing the slope of L_M at infinity with that at unity, it is possible to find a planar angle deficit by

$$\delta/2\pi = 1 - L'_M(\infty) = 0.865. \tag{4.1}$$

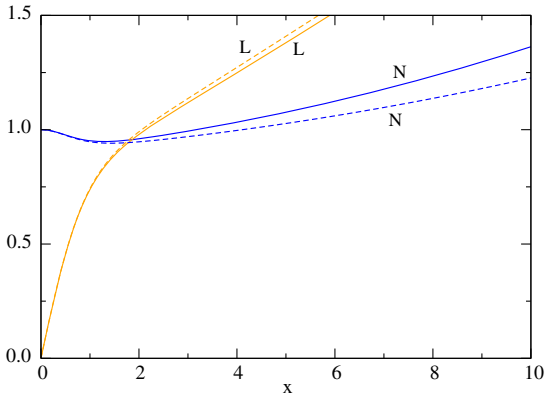

FIG. 6. The metric fields as functions of x for different values of the cosmological constant. For solid lines we adopt $\bar{\Lambda} = -0.010$, and for dashed lines $\bar{\Lambda} = -0.007$. In both plots we consider $\alpha = 0.8, \gamma = 0.6, \beta_2 = 2.0, \beta_3 = 1.0$, and $q = 1.0$.

In Fig. 7(b) we present the behaviors of L and N as functions of x considering the non-Abelian cosmic string in Minkowski and in anti–de Sitter spacetimes. In addition we present their behaviors in the vacuum of anti–de Sitter space. Here also we can see that the main difference in the geometry of the spacetime is given by N: N_{AdS} increases with x while N_M presents a small decay. As for L, we observe that for a given value of x, L_M is bigger than L_{AdS}; moreover, both are smaller that L_{vac}. So, we conclude that the nontrivial structure of the Higgs and gauge fields modify the behavior of L. Specifically the slope of L_{AdS} is smaller than that of L_{vac}.

So, from these two plots, Figs. 7(a) and 7(b), two different observations deserve to be mentioned:

(i) The presence of a cosmological constant affects substantially the geometry of the non-Abelian cosmic string spacetime, modifying mainly the components $g_{tt} = g_{zz}$ of the metric tensor.

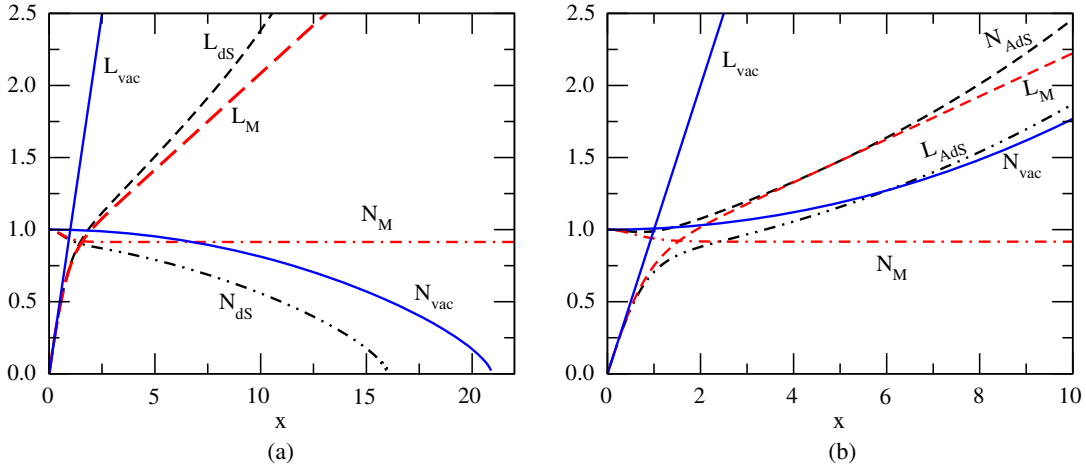

FIG. 7. The metric fields $L(x)$ and $N(x)$ as functions of x. (a) Comparison of the behavior of the metric fields L and N in de Sitter spacetime (dS), considering $\bar{\Lambda} = 0.0075$, with the metric fields in the Minkowski (M) and vacuum (vac) configurations, respectively. (b) Comparison of the behaviour of the metric fields L and N in anti–de Sitter spacetime (AdS), considering $\bar{\Lambda} = -0.03$, with the metric fields in the Minkowski (M) and vacuum (vac) configurations, respectively. In both plots we consider $\gamma = 0.6, \alpha = 0.8, \beta_2 = 2.0, \beta_3 = 1.0$, and $q = 1.0$.

(ii) In the other direction we can see that the presence of the matter field in dS and AdS spaces also produces relevant consequences on the behavior of the metric tensor. Specifically in dS space, the value of the cosmological horizon decreases significantly.

V. CONCLUSION

In this paper, we have examined the influence of the cosmological constant in the geometry of non-Abelian and Abelian cosmic string spacetimes. In agreement with a previous work [27], where the gravitating non-Abelian cosmic strings were studied in the absence of cosmological constant, we have shown that it is also possible to obtain a non-Abelian stable topological string considering two bosonic isovectors with a Higgs mechanism in de Sitter and anti–de Sitter spaces.

Regarding the analysis in de Sitter space, we have shown that there appears a cosmological horizon. In fact, this observation was presented in the paper by Linet for the vacuum configuration in [29] and in [21] for the Abelian string. Here we also returned to this analysis considering both non-Abelian and Abelian strings. These investigations were presented in Figs. 1(b) and 2(b) for specific values of the parameters. By these graphs we have pointed out that the non-Abelian case presents a smaller cosmological horizon than the corresponding Abelian one.

We also provided the behavior of the cosmological horizon, x_0, with the gravitational coupling constant, γ, and with the cosmological constant, $\bar{\Lambda}$. In Fig. 3(a), we can observe that the cosmological horizon decreases when one increases γ. In Fig. 3(b) we can see that the cosmological horizon also decreases for larger values of the cosmological constant. Moreover, we also compare this behavior with the corresponding one for the vacuum case. We see that for a given value of $\bar{\Lambda}$, the horizon associated with the vortex system is smaller than the vacuum one.

The behaviors of the Higgs and gauge fields and metric functions in anti–de Sitter spacetime for the non-Abelian cosmic strings were displayed in Fig. 4. We have also shown the behaviors of Higgs and gauge fields and metric functions for the Abelian cosmic strings in Fig. 5. We noticed that in both cases $N(x)$ diverges for large values of x; however, by our numerical results, we observe that in the non-Abelian case, the slope of $N(x)$ is bigger than the corresponding Abelian one. In Fig. 6, we have shown the behavior of metric fields, N and L, as functions of x for the non-Abelian system considering two different values of $\bar{\Lambda}$. By this graph and others not presented in this paper, we observe that while increasing the cosmological constant, the two lines representing these functions approach each other. This behavior is compatible with the vacuum case.

Finally we have presented in Figs. 7(a) and 7(b) comparative plots of the behaviors of the components $N(x)$ and $L(x)$ of the metric tensor as functions of x, considering the non-Abelian string in Minkowski and de Sitter backgrounds and in Mikowski and anti–de Sitter backgrounds, respectively. We have observed that the presence of the cosmological constant strongly modifies the geometry of the spacetimes produced by the defect. The most relevant modifications are due to the component $N(x)$. For dS, N goes to zero for a finite distance to the string, and for AdS this component increases. Also in these graphs we have presented the behaviors of these two functions in vacuum scenarios. By comparison of the functions in the vacuum scenarios with the full system in dS or AdS, we have observed significant deviations caused by the Higgs and gauge fields in the slopes of L.

ACKNOWLEDGMENTS

E. R. B. M. thanks Conselho Nacional de Desenvolvimento Cientfico e Tecnolgico (CNPq), Process No. 313137/2014-5, for partial financial support. A. d. P. S. would like to acknowledge the Universidade Federal Rural de Pernambuco.

[1] T. W. B. Kibble, J. Phys. A **9**, 1387 (1976).
[2] T. W. B. Kibble, Phys. Rep. **67**, 183 (1980).
[3] A. Vilenkin and E. S. Shellard, *Cosmic Strings and Other Topological Defects* (Cambridge University Press, Cambridge, England, 2000).
[4] P. Ade *et al.* (Planck Collaboration), Astron. Astrophys. **571**, A25 (2014).
[5] M. Hindmarsh, Prog. Theor. Phys. Suppl. **190**, 197 (2011).
[6] E. J. Copeland, L. Pogosian, and T. Vachapati, Classical Quantum Gravity **28**, 204009 (2011).
[7] H. B. Nielsen and P. Olesen, Nucl. Phys. **B61**, 45 (1973).
[8] D. Garfinkle, Phys. Rev. D **32**, 1323 (1985).
[9] P. Laguna-Castillo and R. A. Matzner, Phys. Rev. D **35**, 2933 (1987).
[10] B. Linet, Phys. Lett. A **124**, 240 (1987).
[11] P. Laguna and D. Garfinkle, Phys. Rev. D **40**, 1011 (1989).
[12] M. E. Ortiz, Phys. Rev. D **43**, 2521 (1991).
[13] M. Christensen, A. L. Larsen, and Y. Verbin, Phys. Rev. D **60**, 125012 (1999).
[14] Y. Brihaye and M. Lubo, Phys. Rev. D **62**, 085004 (2000).
[15] D. Kramer, H. Stephani, E. Herlt, and M. MacCallum, *Exact Solutions of Einstein's Field Equations* (Cambridge University Press, Cambridge, England, 1980).
[16] B. Hartmann and J. Urrestilla, J. High Energy Phys. 07 (2008) 006.
[17] J. J. Blanco-Pillado, B. Reina, K. Sousa, and J. Urrestilla, J. Cosmol. Astropart. Phys. 06 (2014) 001.
[18] A. G. Riess *et al.*, Astron. J. **116**, 1009 (1998).
[19] S. Perlmutter *et al.*, Astrophys. J. **517**, 565 (1999).
[20] J. M. Maldacena, Adv. Theor. Math. Phys. **2**, 231 (1998); E. Witten, Adv. Theor. Math. Phys. **2**, 253 (1998); S. S. Gusbser, I. R. Klebanov, and A. M. Polyakov, Phys. Lett. B **428**, 105 (1998).
[21] E. R. Bezerra de Mello, Y. Brihaye, and B. Hartmann, Phys. Rev. D **67**, 124008 (2003).
[22] A. M. Ghezelbash and R. B. Mann, Phys. Lett. B **537**, 329 (2002).
[23] Y. Brihaye and B. Hartmann, Phys. Lett. B **669**, 119 (2008).
[24] M. Barriola and A. Vilenkin, Phys. Rev. Lett. **63**, 341 (1989).
[25] X. Li and J. Hao, Phys. Rev. D **66**, 107701 (2002).
[26] B. Bertrand, Y. Brihaye, and B. Hartmann, Classical Quantum Gravity **20**, 4495 (2003).
[27] A. de Pádua Santos and E. R. Bezerra de Mello, Classical Quantum Gravity **32** (2015) 155001.
[28] H. J. de Vega, Phys. Rev. D **18**, 2932 (1978).
[29] B. Linet, J. Math. Phys. **27**, 1817 (1986).
[30] U. Ascher, J. Christiansen, and R. D. Russel, Math. Comput. **33**, 659 (1979); ACM Trans. Math. Softw. **7**, 209 (1981).